

Supporting Information

Hierarchically structured PtCo nanoflakes-nanotube as electrocatalyst for methanol oxidation

Dongbo Yu,^{a,b} Ezzatollah Shamsaei,^a Jianfeng Yao^a, Tongwen Xu,^b and Huanting Wang^{*a}

^a Department of Chemical Engineering, Monash University, Clayton, Victoria 3800, Australia

^b CAS Key Laboratory of Soft Matter Chemistry, Laboratory of Functional Membranes, School of Chemistry and Materials Science, University of Science and Technology of China, Hefei, Anhui, 230026, People's Republic of China

E-mail addresses: huanting.wang@monash.edu

Tel: +61 3 9905 3449; Fax: +61 3 9905 5686

Experimental section

Materials Synthesis

Branched Co₃O₄ nanowire array was prepared by using our previously reported method.¹ Co metal nanowire cluster was prepared by annealing the branched Co₃O₄ nanowire array at 450°C with H₂ flow for 2h. The obtained Co nanowire cluster on Ni foam with 1 cm² in area was then directly immersed into a certain volume of H₂PtCl₆ aqueous solution (0.5 mg/ml) overnight to get PtCo nanoflakes-nanotube. The resulting electrodes were denoted as PtCo-X, where X was the theoretically loading amount of Pt and specified to be 0.2, 0.4, 0.6, 0.8, 1.0, 2.0 and 2.5 mg. For comparison, orderly aligned Co metal nanowire array (OA-Co NA) was used as the precursor materials for fabricating the similar PtCo nanoflakes-nanotube (OA-PtCo-X). To follow the similar synthesis procedure, only straight Co₃O₄ nanowire array was the starting material in the preparation process of OA-Co NA (annealing at 350°C), and the detailed synthesis of straight Co₃O₄ nanowire array was described in the previous study.¹ In addition, for less-dense OA-PtCo-X, the as-prepared straight Co₃O₄ nanowire array template was first treated with ultrasonic bath for 15 seconds,

in order to obtain sparse distribution of Co₃O₄ nanowire array.

Structure and electrochemistry characterizations

The structure and morphology of PtCo nanoflakes-nanotube were characterized by using a scanning electron microscope (SEM, JEOL JSM-6300F) and a transmission electron microscope (TEM, JEM-2100) operated at 200 KV. The elemental analysis of PtCo nanoflakes-nanotube was examined by an energy dispersive X-ray spectrometer (EDS) attached to the TEM (JEM-2100). The X-ray diffraction (XRD) was conducted on a Bruker D8 Advance X-ray diffractometer with Cu K α radiation. The X-ray photoelectron spectroscopy (XPS) analyses were examined on a Thermo Fisher X-ray photoelectron spectrometer system (ESCALAB250). The electrochemical tests were investigated by cyclic voltammetry (CV), linear sweep voltammetry (LSV), chronoamperometry and electrochemical impedance spectroscopy (EIS) in 2 M NaOH aqueous solution using an Autolab 2 instrument (Metrohm Autolab B.V., The Netherlands) at room temperature. EIS analysis was measured ranging from 0.1Hz to 100 kHz at open-circuit potential with an ac perturbation of 0.1 V. KCl saturated Ag/AgCl and graphite rod were used as reference electrode and counter electrode, respectively, and the nickel foam supported electroactive catalysts ($\sim 1 \text{ cm}^2$) were directly used as the working electrode. For comparison, the working electrode for commercial Pt/C and PtRu/C (20 wt%, Sigma Aldrich) was also prepared, a mixture solution composed of 20 mg of Pt/C or PtRu/C, 100 μl Nafion solution ($\sim 5\%$ in a mixture of lower aliphatic alcohols and water, Sigma Aldrich) and 0.9 ml ethanol was ultrasonicated for 60 min. The mixed solution was then dispersed on 1 cm^2 of carbon paper (TGPH-030, Toray), yielding a catalyst loading amount of 0.4 mg/cm^2 , and finally dried at 80 $^\circ\text{C}$ for 1 h in air. The CO stripping test was conducted on the base of LSV measurements. O₂ dissolved in 2 M NaOH solution was removed by bubbling N₂ gas for 15 min, and the electrolyte solution was then saturated by bubbling CO gas for 15 min and finally treated with N₂ gas bubbling again.

Energy, 2014, **10**, 153-162.

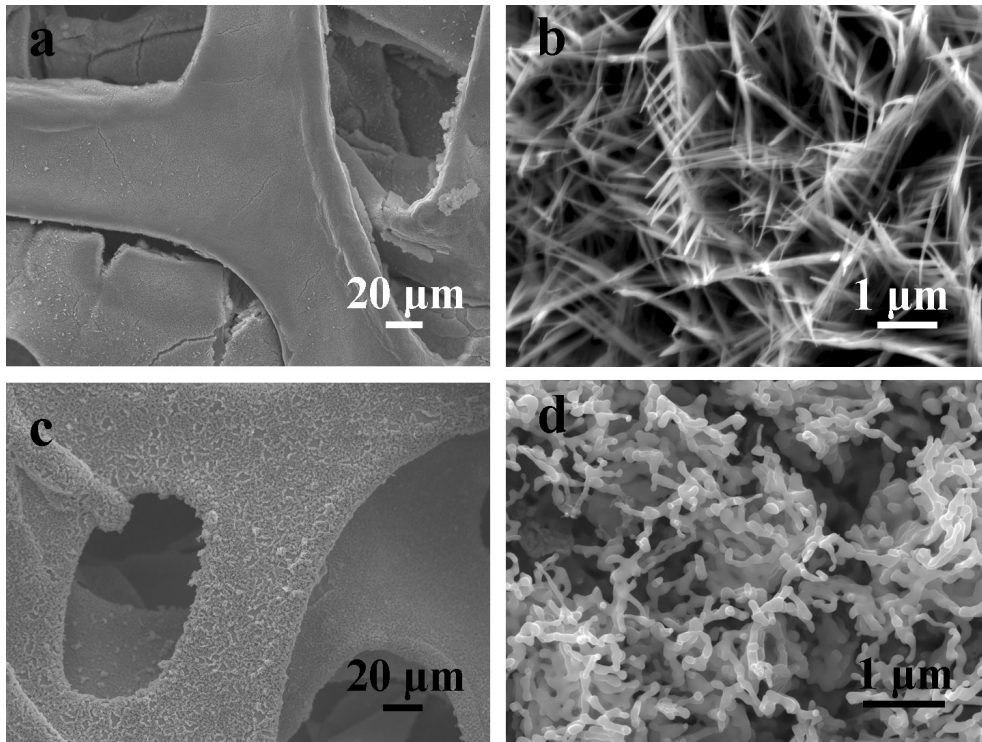


Figure S1 SEM images of branched Co_3O_4 nanowires (a, b) and Co nanowire cluster (c, d) on Ni foam.

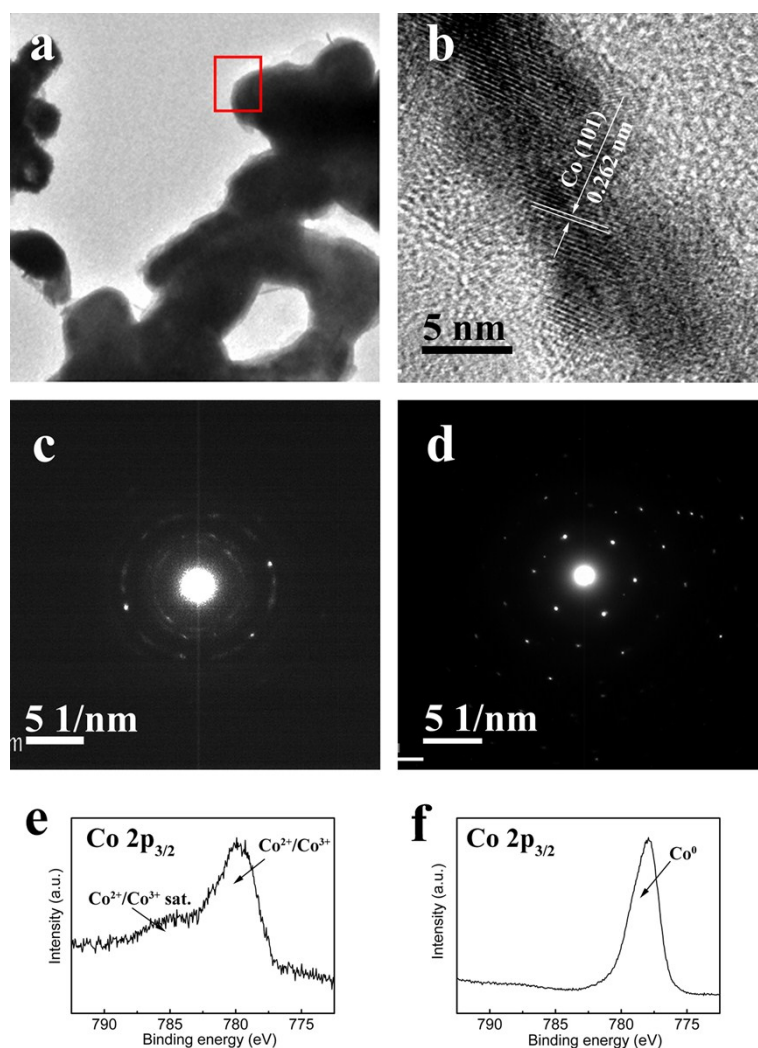


Figure S2 TEM image (a) and high-resolution image (b) of Co nanowires; electron diffraction (ED) patterns in selected areas (c, d), d zooms in on the red rectangle area of a; high-resolution XPS spectra of Co 2p_{3/2} of Co₃O₄ nanowires (e) and Co nanowires (f). The Co nanowires had a smooth surface (a), and the lattice spacing of 0.262 nm corresponded to Co(101) plane (b) that was close to 0.23 nm of PtCo(111), this would cause strain dislocations at the interface between Co nanowire and new formed PtCo, which may induce the growth of PtCo with nanoflake structure. The ED pattern of Co nanowires demonstrated diffraction rings, indicating the polycrystalline structure; meanwhile, if zoomed in a small-scale area, it showed a single-crystal diffract spot, that's because the porous Co₃O₄ nanowire precursor was actually composed of numerous small nanoparticles, each nanoparticle may convert into an

individual single-crystal Co nanoparticle, they were melt together into a solid nanowire during the reduction reaction, in agreement with the observation of shrinkage of diameter after reduction reaction. It could be clearly seen the $\text{Co}^{2+}/\text{Co}^{3+}$ band (~ 780 eV) and its satellite band (~ 785 eV) in the high-resolution XPS spectra of Co $2p_{3/2}$ of Co_3O_4 nanowires clearly (e); in contrast, the Co nanowires only presented a Co^0 band located at ~ 791.1 eV (f), implying the complete transformation in H_2 gas flow.

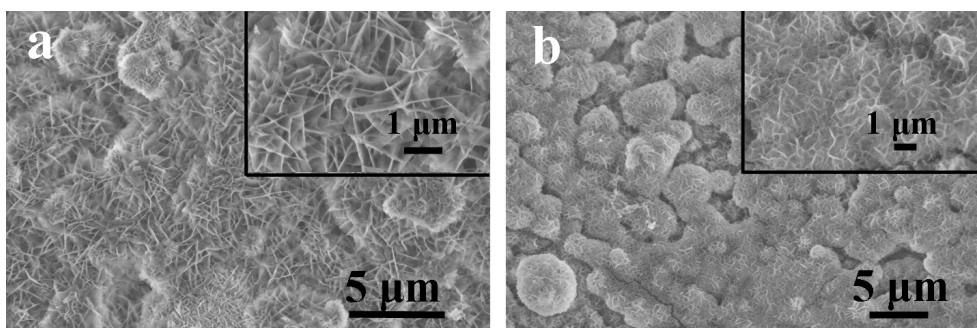


Figure S3 SEM images of CoPt-2.0 (a) and CoPt-2.5 (b). The insets show their corresponding high-magnification SEM images.

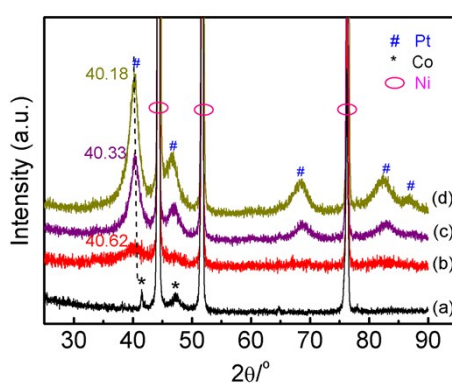


Figure S4 XRD patterns of Co nanowire (a), PtCo-0.2 (b), PtCo-0.4 (c) and PtCo-0.8 (d)

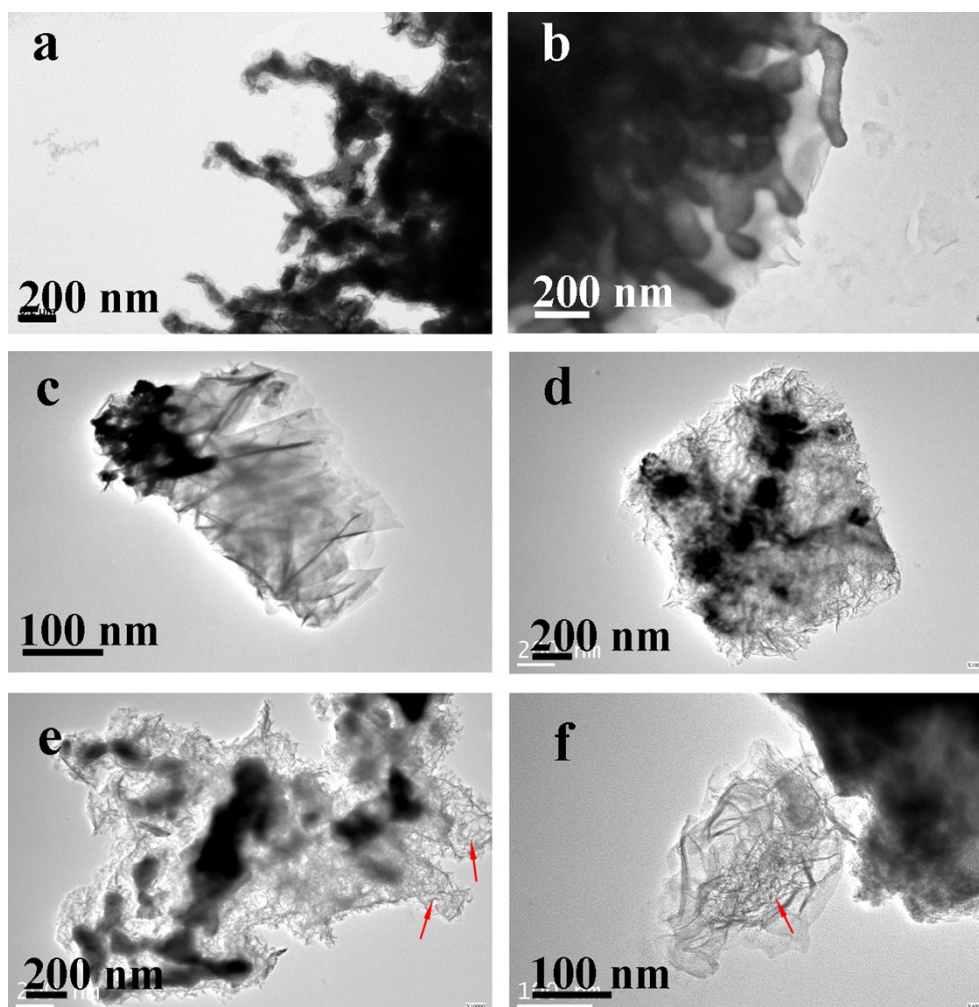


Figure S5 TEM images of PtCo-0.4 (a) and PtCo-0.8 (b-f). The red arrows in (e) and (f) show the hollow tubular morphology of nanoflakes-nanotube structure.

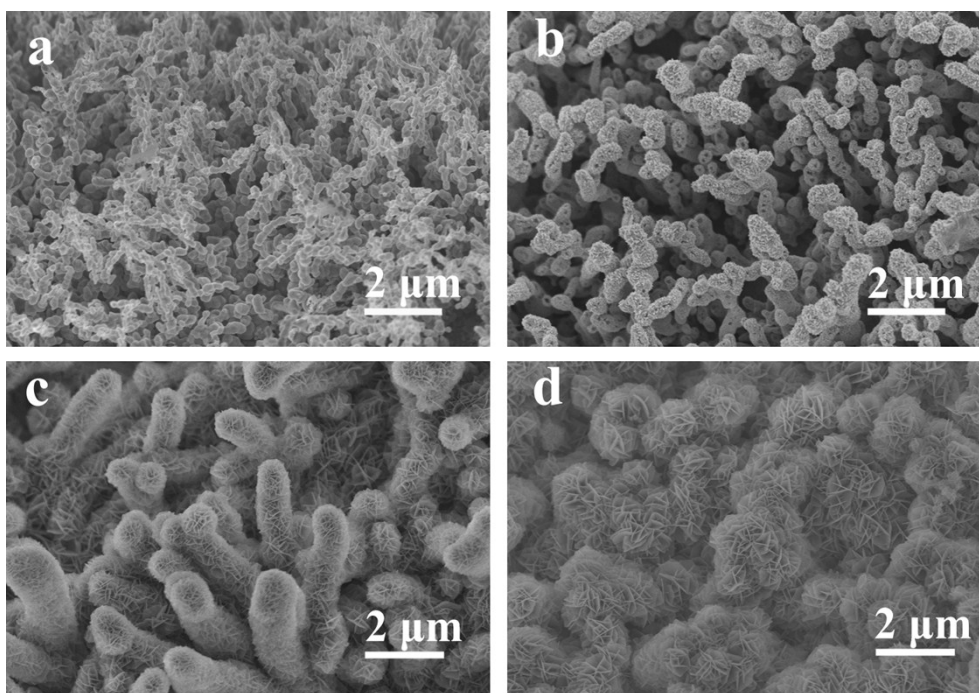


Figure S6 SEM images of PtCo-0.8 as a function of reaction time: 1 h (a), 4 h (b), 8 h (c) and 12 h (d).

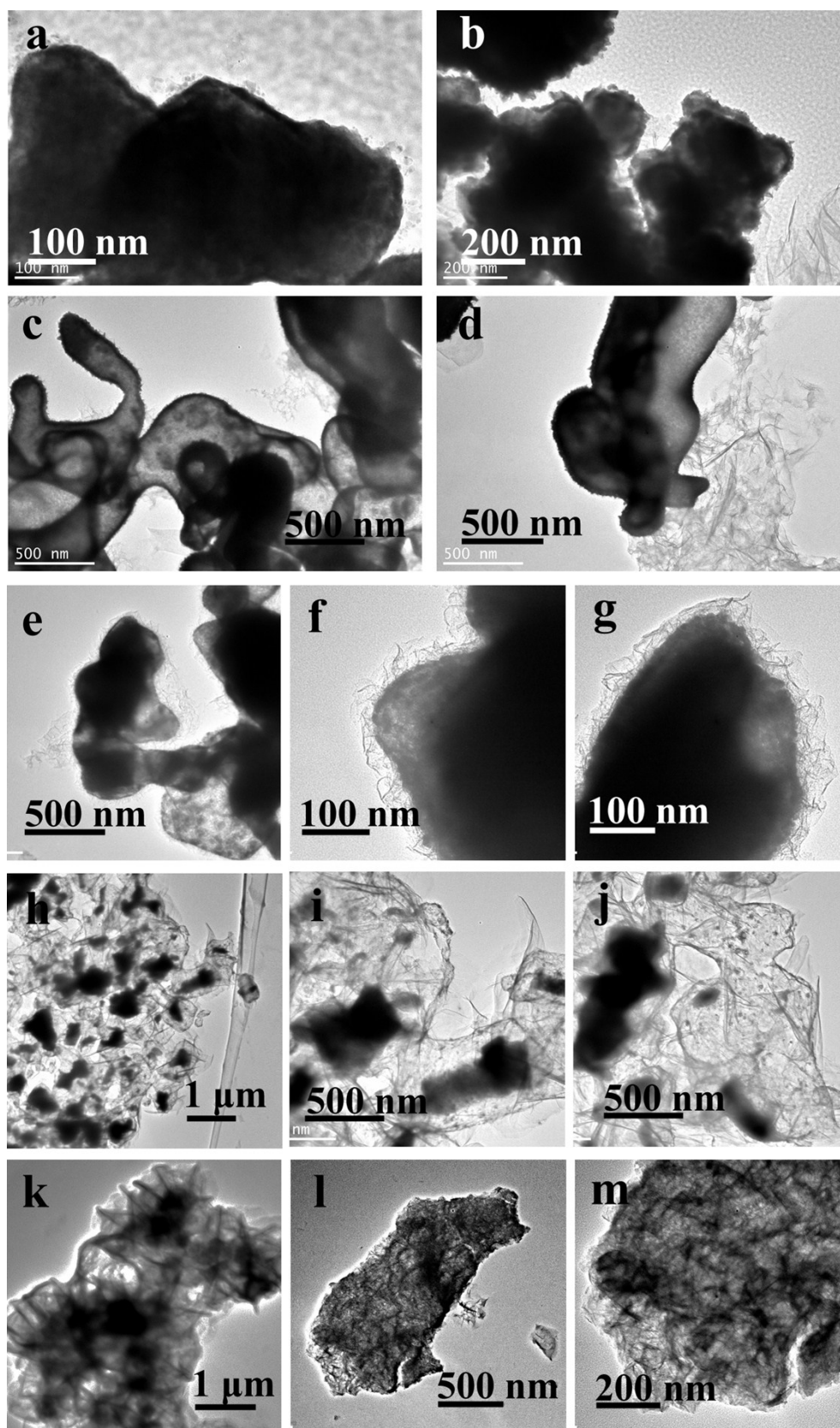


Figure S7 TEM images of PtCo-0.8 as a function of reaction time: 2 h (a, b), 4 h (c-g), 8 h (h-j) and 12 h (k-m).

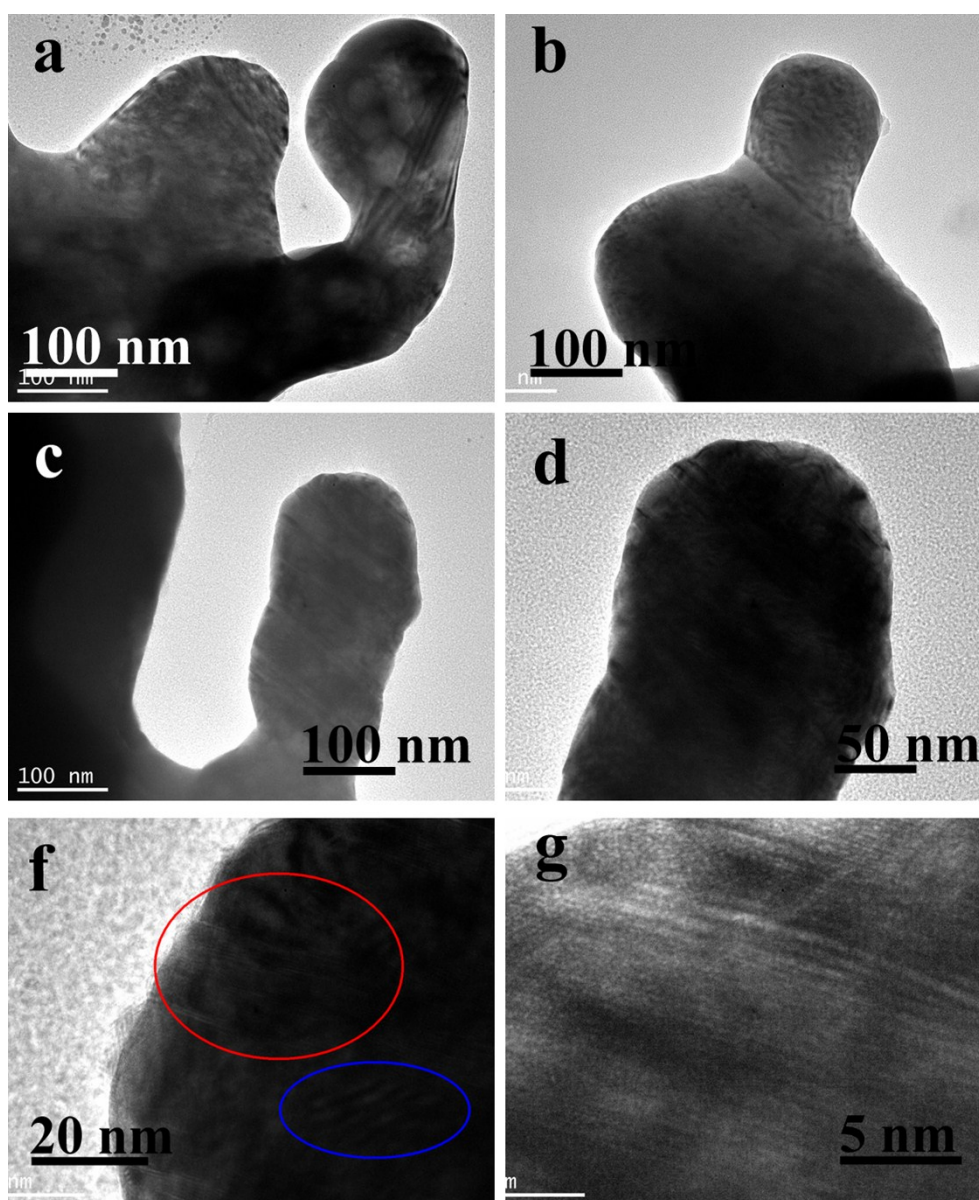


Figure S8 TEM images of PtCo-0.8 after reaction for 1 h. It is clear to see the formation of moiré fringe-like structures (a-d), which was attributed to the difference between crystalline lattices of Co and Pt, resulting in the strain-relief pattern on the surface of Co nanowires. The different crystalline lattice parameter also caused the broadening crystalline interspacing of Co base metal.

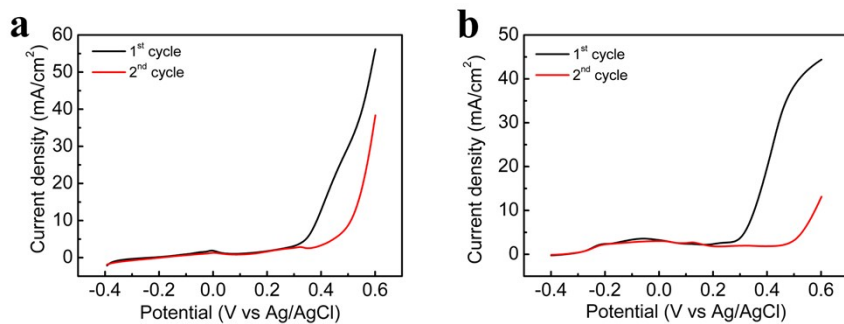


Figure S9 CO stripping voltammetry of Co metal nanowire arrays in 2 M NaOH aqueous solution at a scan rate of 5 mV/s. The CO was pre-absorbed at 0 V for 15 min. Two Co metal nanowire array samples were examined. It is clear that the CO stripping for Co metal nanowire was different from that of Pt. A wave peak appeared rather than the sharp peak of Pt catalyst, indicating that the CO stripping occurred with the transformation from Co(OH)_2 to CoOOH , and the formed CoOOH assisted in oxidizing CO to CO_2 ranging from 0.3 ~ 0.55 V.

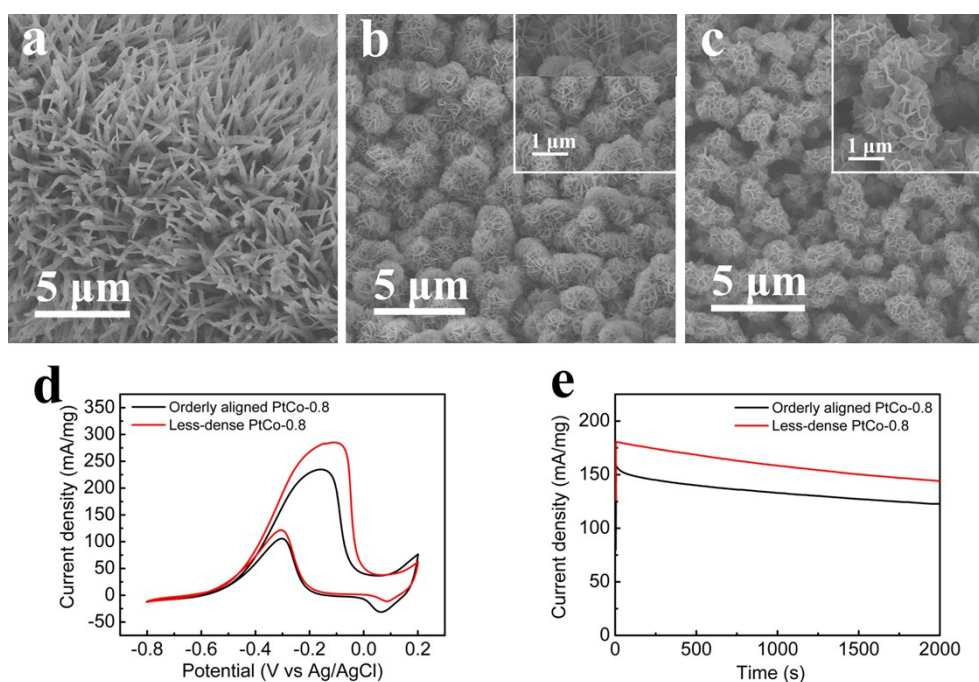


Figure S10 SEM images of orderly aligned Co metal nanowire array (a), OA-PtCo-0.8 (b) and less-dense OA-PtCo-0.8 (c); CV plots of OA-PtCo-0.8 and less-dense OA-PtCo-0.8 in 2 M NaOH + 1 M methanol at a scan rate of 5 mV/s (d) and their corresponding chronoamperometry curves at -0.2 V (e). If the as-obtained Co_3O_4 nanowire array was used as the precursor for the synthesis of OA-PtCo-0.8, the distribution of orderly aligned Co metal nanowire array (a) was so dense that the architecture of resulting OA-PtCo-0.8 (b) could be similar to that of PtCo-0.8; the interspaces among nanoflakes-nanotube unit were still very narrow. With the ultrasonic treatment of dense Co_3O_4 nanowire array for 15 seconds, part of Co_3O_4 nanowires could be peeled off from Ni foam substrate, leading to less-dense distribution of Co_3O_4 and thus the successful preparation of less-dense OA-PtCo-0.8. Due to the more favorable configuration that boosted the transport efficiency and offered more catalytic sites, the less-dense OA-PtCo-0.8 exhibited better electrocatalytic activity and stability for methanol oxidation. In addition, the common OA-PtCo-0.8 showed a bit lower activity than branched Co_3O_4 -derived PtCo-0.8. The results suggested that tuning the catalysts with smart structure was very preferable.

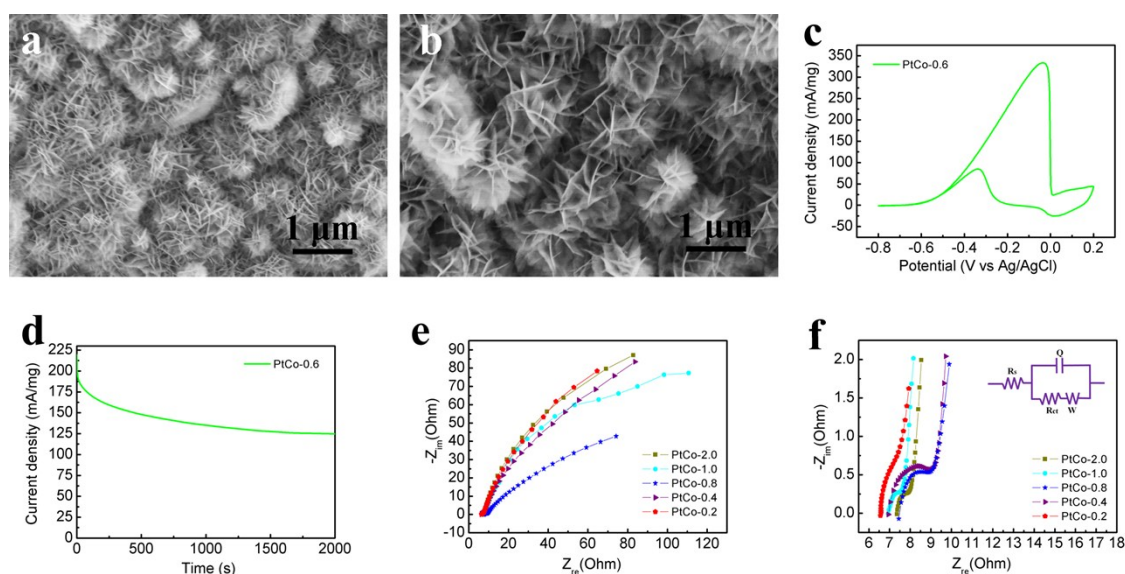


Figure S11 SEM images (a, b) of PtCo-0.6; CV curve of PtCo-0.6 in 2 M NaOH + 1 M methanol at a scan rate of 5 mV/s (c) and its corresponding chronoamperometry curve at -0.2 V (d); EIS plots of PtCo-0.2, PtCo-0.4, PtCo-0.8, PtCo-1.0 and PtCo-2.0 after 2000 s chronoamperometry measurements ranging from 0.1Hz to 100 kHz (e), enlarged EIS plots at low frequency (f). The equivalent electrical circuit (inset of Figure S6f) contains electrolyte solution resistance (R_s), charge transfer resistance (R_{ct}), Warburg impedance (W) and constant phase element (Q).

Table S1 The values extracted from Fig. 4, Figure 10d-e and Figure S11c-d.

Catalyst	Current density of cyclic voltammetry (mA/mg)				Current density of chronoamperometry at -0.2 V		
	onset potential (V)	forward scan (I _f)	backwa rd scan (I _b)	the ratio of I _f /I _b	at 0 s (mA/mg)	at 2000 s (mA/mg)	stability (%)
20% Pt/C	-0.61	149.8	70.3	2.13	68.1	47.2	69.3%
20% PtRu/C	-0.68	189.1	48.3	3.91	112.3	87.3	77.8%
PtCo-0.2	-0.64	187.7	44.8	4.19	165.0	39.1	23.7%
PtCo-0.4	-0.69	259.5	69.8	3.71	167.2	93.4	55.8%
PtCo-0.6	-0.70	332.7	83.5	3.98	199.8	126.4	63.3%
PtCo-0.8	-0.67	253.4	82.1	3.08	149.0	120.9	81.1%
PtCo-1.0	-0.62	156.0	61.3	2.54	91.9	76.1	82.8%
PtCo-2.0	-0.57	65.4	20.8	3.14	49.7	39.6	79.7%
PtCo-5.0	-0.55	55.4	18.1	3.07	25.4	20.8	81.9%
OA-PtCo-0.8	-0.67	236.7	104.6	2.26	155.7	123.1	79.1%
Less-dense OA-PtCo-0.8	-0.69	287.3	120.7	2.38	181.7	145.3	79.9%

Table S2 The calculated R_{ct} values extracted from Figure S11f.

Electrode	PtCo-0.2	PtCo-0.4	PtCo-0.8	PtCo-1.0	PtCo-2.0
R _{ct} (Ω)	2.98	2.51	1.62	0.83	0.78